COUPLING OF MACROSCALE AND NANOSCALE SIMULATIONS OF SOOT FORMATION IN A DIFFUSION FLAME

J. Morán[1], F. Escudero[2], A. Fuentes[2], A. Poux[1], F. Cepeda[3], L. Gallen[4], E. Riber[4], and J. Yon*[1]

[1]Normandie Univ., UNIROUEN, INSA Rouen, CNRS, CORIA, 76000 Rouen, France
[2]Dep. de Industrias, Univ. Técnica Federico Santa María, Av. España 1680, Casilla 110-V, Valparaíso, Chile
[3]Department of Mechanical and Industrial Engineering, Ryerson University, M5B 2K3, Toronto, Canada
[4]CERFACS, 42 avenue Gaspard Coriolis, Toulouse 31047, France
*Courriel de l'orateur : yon@coria.fr

TITRE

Couplage de simulations à l'échelle macro et nanométrique de la formation de suie dans une flamme de diffusion

RESUME

Des études expérimentales ont suggéré que les particules de suie formées le long de différentes lignes de courant dans une flamme de diffusion peuvent avoir des morphologies différentes. Cependant, les incertitudes liées à l'échantillonnage et à leur analyse rendent difficile la quantification de ces différences. Dans ce travail, ce problème est exploré d'un point de vue numérique grâce à un couplage de simulations aux échelles macroscopique et nanoscopique. Ces simulations montrent des agrégats remarquablement plus grands et plus compacts dans les ailes de la flamme comparativement à ceux rencontrés le long de l'axe central. L'analyse des paramètres morphologiques tels que l'anisotropie, le recouvrement des monomères et le nombre de coordinance révèle la compléxité de la morphologie des particules de suie ainsi que la présence d'agrégats en chaîne le long des différentes lignes de courant de la flamme.

ABSTRACT

Experimental studies have suggested that soot particles formed along different streamlines in a diffusion flame may have different morphologies. However, the uncertainties linked to the sampling and their analysis make difficult the quantification of these morphological differences. This work explores this problem from a numerical point of view thanks to a coupling of nanoscale and macroscale simulations. The coupling shows remarkably larger and more compact aggregates near the wings of the flame compared to its centerline. The analysis of morphological parameters such as anisotropy, monomers overlapping, and coordination number reveals the complex morphology of soot and shows the presence of chain-like aggregates along the different streamlines of the flame.

MOTS-CLÉS : MET, suie, morphologie, recouvrement / **KEYWORDS:** TEM, soot, morphology, overlapping

1. INTRODUCTION

The macroscopic Computational Fluid Dynamics (CFD) approach, such as CoFlame (Eaves et al., 2016). allows the dynamics of flames to be simulated by including the mass, momentum, and energy balance. In this context, the aerosol phase is treated based on the Population Balance Equation (PBE). This approach is widely used in different applications spanning aerosol, powders, and combustion systems. However, PBE calculations assume the morphology of particles, generating significant uncertainties related to the particle formation dynamic and their transport modeling. For instance, experimental measurements have suggested that soot particles may have a different morphology depending on their formation along different streamlines in the flame (Kholghy et al., 2013; Chu et al., 2019). However, the uncertainties in sampling and post-processing the data did not enable a quantitative description, and no numerical simulations have hitherto been able to verify these findings.

On the other hand, the morphology of soot particles formed under flame conditions is often explained by the classical diffusion-limited agglomeration process. However, these codes are not adapted to study the time-dependent evolution of particles in flames and do not include the surface reactions that considerably influence the morphology of aggregates. Recently, a new nanoscale approach to simulate soot aggregation induced by the Brownian motion, which considers change of flow regimes and surface reactions, has been introduced (Morán et al., 2021a). This approach allows the detailed morphology of soot particles to be studied. Nonetheless, this code is (by definition) not able to simulate the dynamics of the flame gas phase. Therefore, a macroscopic-nanoscopic coupling approach is currently needed. This work intends to fill this gap of knowledge by coupling these two types of codes.

2. METHODOLOGY

2.1. CFD macroscale flame simulations

The target flame corresponds to a laminar diffusion flame generated by a Gülder burner. The fuel (ethylene) is injected in a central tube (10.9 mm and 12.7 inner and external diameter, respectively) at 0.194 l_n/min flowrate, and oxidizer (air) is injected in the 90 mm inner diameter coflow tube at 150 l_n/min flowrate. This flame is simulated by a macroscopic approach using CoFlame (Eaves *et al.*, 2016). This code has been extensively used in the literature to study laminar premixed and mainly diffusion flames. In this code, the conservation of mass, momentum, energy, and species mass fractions is solved in a 2-dimensional coordinate system (radial r and axial z), possible thanks to the axisymmetric flame configuration. A 5-rings Polycyclic Aromatic Hydrocarbon (PAH) model is used to predict soot particles nucleation and condensation. The aerosol phase is taken into account thanks to the solution of the PBE for the aggregates and primary particles number concentrations solved using a fixed sectional method (Eaves *et al.*, 2016).

2.2. Data extraction for nanoscale simulations

Coupling macroscopic and nanoscopic simulations require the determination of soot particles trajectories through the flame. A Lagrangian approach determines these trajectories. To this end, Newton's law of linear momentum conservation is numerically solved for a spherical tracer considering the drag and thermophoretic forces. For a selected Lagrangian trajectory of soot particles in the flame, the CFD code provides two necessary inputs for nanoscale simulations, including (1) the initial conditions and (2) the time-dependent properties. The former involves the initial primary particle size distribution and volume fraction. The time-dependent properties include: the local flame temperature, the nucleation mass flux (kg/m^3/s), and the net surface reactions (HACA surface growth, PAH condensation, and oxidation) flux (kg/m^3/s).

2.3. Nanoscale simulations

They are carried out using the recently introduced Monte Carlo Aggregation Code (MCAC) (Morán *et al.*, 2020). This code has been used to study soot aggregation and surface growth (Morán *et al.*, 2021a). In this work, MCAC has been adapted to consider the temporal evolution of nucleation, soot oxidation, and oxidation-induced fragmentation. This code has also been adapted for coupling with macroscale CFD codes by considering both the initial conditions and the time-dependent properties provided by the macroscopic approach. MCAC simulates the positions of particles experiencing a Brownian motion that sticks together upon collisions, thus forming aggregates in a cubic box. At the same time, new isolated primary particles can be injected into the box to simulate soot nucleation and primary particles radius increases due to surface growth or decrease due to the oxidation process. When oxidation takes place, each primary particle diameter whose diameter is below a minimum critical (D_c) are considered to be completely consumed by oxidation, and therefore they are deleted from the simulation domain. Also, all the pairs of monomers connected within aggregates are checked, with primary particles that are no longer in contact due to oxidation being separated in an aggregate fragmentation process. A minimum critical diameter $D_c = 5$ nm is considered. Below this diameter, soot particles are considered to behave like a cluster of molecules whose dynamics are beyond the scope of this work. Soot particles are considered to be mature, having a bulk density $\rho_p = 1.9$ g/cm^3. Their collision and sticking probabilities are considered unitary (Morán *et al.*, 2021b).

3. RESULTS

On the left-hand side of **Fig. 1**, the soot volume fraction field as simulated by CoFlame is shown. These volume fractions show a maximum value close to 8 ppm, which is moderately underestimated when compared with the maximum of 13 ppm recently found in experiments carried out under exactly the same flame conditions (Yon *et al.*, 2021a). However, the spatial distribution of the volume fraction is in excellent agreement with the referred work. Flame temperature is also in excellent agreement with the referred work. The same figure also reports the four selected Lagrangian trajectories, including the centerline (in red), the intermediate-1 (in orange), the intermediate-2 (in violet), and the wings (in black). As observed in the figure, the centerline and the wing trajectories are selected due to passing respectively through the zones of minimum and maximum soot volume fractions, and the other two trajectories are selected for being intermediate cases between these two extremes.

On the right-hand side of **Fig. 1**, numerical Transmission Electron Microscopy (nTEM) images are shown. These images are obtained by sampling aggregates at every 10 mm along the axial position z from MCAC simulations for the four selected trajectories. All the images have the same size and resolution, as indicated on the top right-hand side of the figure. From the observation of these figures, different conclusions can be obtained. First, soot aggregates formed along the centerline and intermediate-1 trajectory seem much smaller and spherical-like than those formed along other trajectories. Second, when observing the evolution of particles along the same trajectory, different soot formation processes can be identified. At the lowest axial position,
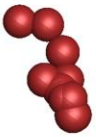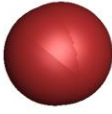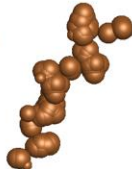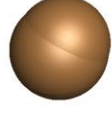
particles are small but still observable even in the regions of low volume fraction (below 0.5 ppm). This is explained by the different zones in the flame where nucleation is more intense; for instance, nucleation rates are high but eminently concentrated in space at a radial position around 5 mm and axial position z~1 mm. Similarly, it is also quite intense but spatially dispersed around $15 < z < 20$ mm, and $0 \leq r < 1.8$ mm (see Fig. D15 from Yon *et al.*, 2021b). By observing higher axial positions, larger primary particles and aggregates are observed due to agglomeration and surface growth. Finally, at the highest z of each trajectory, both primary particle and aggregate size are smaller due to oxidation and fragmentation.
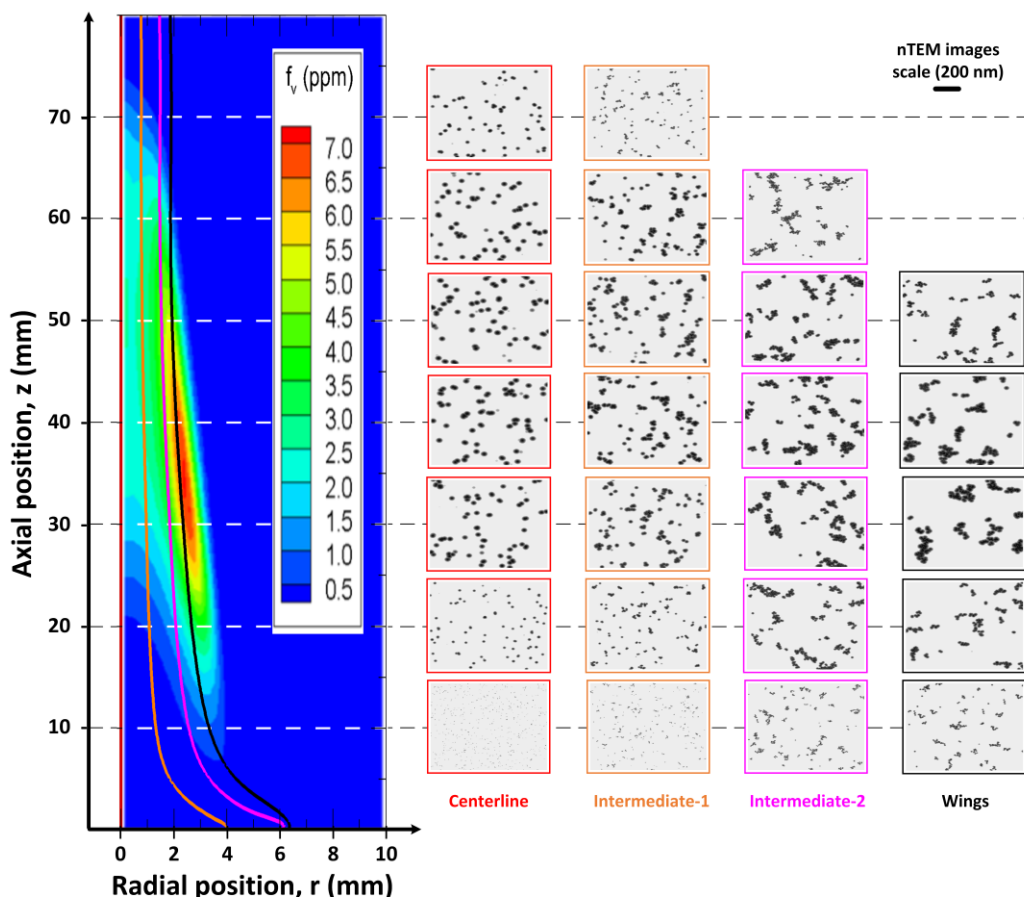
Figure 1: Numerical Transmission Electron Microscopy images of soot particles formed along the selected trajectories.

Fig. 2 reports some examples of aggregates with extreme morphological properties, including the effective number of primary particles ($N_{\mathrm{p,eff}}$), anisotropy coefficient (A_{13}), aggregate's mean overlapping coefficient (c_{ov}), and aggregate's mean coordination number (n_c). Additional parameters such as the primary particle polydispersity ($\sigma_{Dp,geo}$), the specific surface area (S_s), and the radius of gyration (R_g) are also reported for each aggregate shown in this figure. The largest number of effective primary particles per aggregate is $N_{\mathrm{p,eff}} = 59$, found in the intermediate 2 trajectory at $z = 40$ mm. This shows the huge difference with those aggregates formed along the centerline, where a maximum of $N_{\mathrm{p,eff}} = 7.4$ is found. The population-averaged anisotropy coefficient is between 1.4 and 2.6, larger for those aggregates formed alongside the intermediate 2 and in the wings compared to other trajectories. However, the maximum values observed for individual aggregates are between 9.5 to 15.8 found in the centerline and intermediate 2 trajectory, respectively. These values are mainly determined by aggregation and not highly affected by surface reactions. This shows that chain-like aggregates can be found along the different streamlines of the flame, but their sizes are considerably different when depending on the trajectory of particles in the flame. Maximum overlapping coefficients as high as 93% were observed for dimmers. These particles seem spherical and may be easily confused with isolated primary particles in experimental TEM image analysis as indeed they show $N_{\mathrm{p,eff}} \to 1$. The primary particle coordination number can reach 34, whereas it has been found to be lower than 17 for aggregates produced in premixed flames (Morán *et al.*, 2021a). Also, the population-averaged values tend toward 2 for agglomerates made of point-touching primary spheres formed by diffusion-limited aggregation process. Interestingly, when selecting the aggregates showing the maximum primary particle coordination number, very compact aggregates are observed whose morphology is different from that of aggregates showing the maximum c_{ov}. This shows the

high impact of surface growth on the local compactness of aggregates as especially revealed by those formed in the intermediate trajectories.

Figure 2: Examples of aggregates with extreme morphological parameters including, maximum effective number of primary particles per aggregate, maximum anisotropy, maximum aggregate's overlapping, and maximum aggregate's coordination number found for each trajectory.

4. CONCLUSIONS

A Lagrangian tracking approach has been implemented to couple macroscopic and nanoscopic codes to study the detailed morphological evolution of soot particle in an ethylene flame. The size and morphology of particles formed along different streamlines in the flames are remarkably different. Particles formed in the wings of the flame are much larger and show a higher degree of local compactness than the centerline of the flame.

ACKNOWLEDGMENTS

REFERENCES

Chu, H., *et al.* (2019). Experimental investigation of soot morphology and primary particle size along axial and radial direction of an ethylene diffusion flame via electron microscopy. *Journal of the Energy Institute*, *92*(5), 1294-1302.

Eaves, N. A., *et al.* (2016). CoFlame: A refined and validated numerical algorithm for modeling sooting laminar coflow diffusion flames. *Computer Physics Communications*, 207, 464-477.

Kholghy, M., Saffaripour, M., Yip, C., & Thomson, M. J. (2013). The evolution of soot morphology in a laminar coflow diffusion flame of a surrogate for Jet A-1. *Combustion and Flame*, *160*(10), 2119-2130.

Morán, J., Yon, J., & Poux, A. (2020). Monte Carlo Aggregation Code (MCAC) Part 1: Fundamentals. *Journal of Colloid and Interface Science*, *569*, 184-194.

Morán, J., Poux, A., & Yon, J. (2021a). Impact of the competition between aggregation and surface growth on the morphology of soot particles formed in an ethylene laminar premixed flame. *Journal of Aerosol Science*, *152*, 105690.

Morán, J., Henry, C., Poux, A., & Yon, J. (2021b). Impact of the maturation process on soot particle aggregation kinetics and morphology. *Carbon*, *182*, 837-846.

Yon, J., *et al.* (2021a). Revealing soot maturity based on multi-wavelength absorption/emission measurements in laminar axisymmetric coflow ethylene diffusion flames. *Combustion and Flame*, 227, 147-161.

Yon, J., *et al.* (2021b). Horizontal Planar Angular Light Scattering (HPALS) characterization of soot produced in a laminar axisymmetric coflow ethylene diffusion flame. *Combustion and Flame*, *232*, 111539.